RECENT PERFORMANCE OF THE ANL ECR CHARGE BREEDER*

R. Vondrasek, R. Scott, R. Pardo, A. Kolomiets, ANL, Argonne, IL 60439, U.S.A.

Abstract

The construction of the Californium Rare Ion Breeder Upgrade (CARIBU) [1], a new radioactive beam facility for the Argonne Tandem Linac Accelerator System (ATLAS), is complete and the project is now in the commissioning phase. The facility will use fission fragments, with charge 1+ or 2+, from a 1 Ci ^{252}Cf source; thermalized and collected into a low-energy particle beam by a helium gas catcher. An existing ATLAS ECR ion source was modified to function as a charge breeder in order to raise the ion charge sufficiently for acceleration in the ATLAS linac. A surface ionization source and an RF discharge source provide beams for charge breeding studies. An achieved efficiency of 11.9% for ^{85}Rb^{19+}, with a breeding time of 200 msec, and 15.6% for ^{84}Kr^{17+} has been realized. Both results are with the source operating with two RF frequencies (10.44 + 11.90 GHz). After modification to the injection side iron plug, the charge breeder has been operated at 50 kV, a necessary condition to achieve the design resolution of the isobar separator.

ECR CHARGE BREEDER

The charge breeder is a room temperature ECR ion source with an open structure NdFeB hexapole with a wall field of 0.86 T [2]. The open hexapole structure allows for pumping through the six 17 mm x 41 mm radial slots, resulting in a source pressure of 2x10^{-8} mbar without plasma and 8x10^{-8} mbar with plasma. The pressure in the extraction region is typically 4x10^{-8} mbar. The source is capable of accepting multiple frequencies with the RF launched through the hexapole radial slots. This scheme allows a large amount of iron to be retained on the injection side of the source resulting in a high magnitude and symmetric axial field. The low charge state ions are introduced into the plasma through a stainless steel tube mounted on a linear motion stage which has a 30 mm range of travel. This allows the deceleration point of the low charge state ions to be adjusted on line without disturbing the source conditions.

Injection Region Modifications

For the isobar separator to achieve the required resolution of 1:20,000, beam extraction from the gas catcher must occur at 50 kV. Hence, the high voltage isolation of the source was upgraded to allow 50 kV operation. However, penning discharges in the injection region occurred at 30 kV bias. An iron plug in this region was modified to increase the gap size from 6.5 mm over a 100 mm length to 10.8 mm at a discrete location as shown in Fig. 1. After several weeks of conditioning, the source operates reliably at 50 kV.

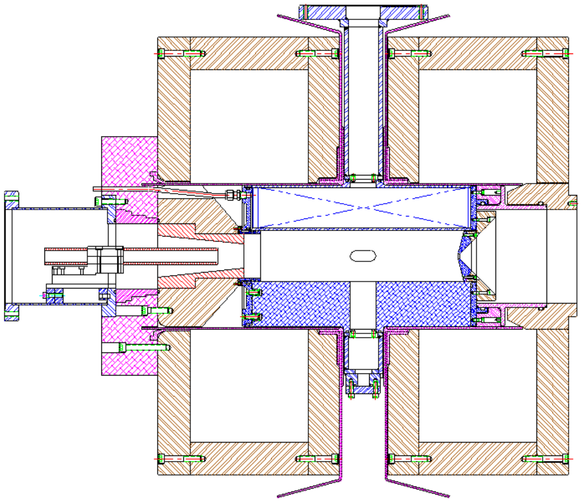

Figure 1: Schematic of the ANL ECR charge breeder. The 1+ beam is injected from the left via the transfer tube. The iron plug which was modified is highlighted with diagonal red. The radial slots where the RF is launched are visible on the source mid-plane.

CHARGE BREEDING RESULTS

The 1+ beam is mass analyzed and injected into the ECR source via a grounded transfer tube. The ions decelerate into the plasma region where a sub-set of them are ionized and captured by the plasma [3].

It was observed that the tune of the 1+ injection line was critical for breeding efficiency. For beams from elemental solids, the optimum injection channel was extremely narrow with a high degree of sensitivity to the entrance einzel lens. With gaseous elements, the einzel lens setting was not as critical, but steering constraints remained very stringent. The position of the transfer tube was also found to be an important variable. A summary of achieved charge breeding efficiencies is given in Table 1. The breeding time was measured by pulsing the incoming 1+ beam and measuring the n+ response time.

Table 1: Summary of charge breeding results.

Ion Species	**n+ Charge State**	**Efficiency (%)**	**Breeding Time (msec)**
Kr-86	17+	15.6	-
Rb-85	19+	11.9	200
Xe-129	25+	13.4	~250
Cs-133	20+	2.9	-

---

* This work was supported by the U.S. Department of Energy, Office of Nuclear Physics, under Contract No. DE-AC02-06CH11357.

Position of the Transfer Tube

In previous work, it was found that the breeding efficiency increased as the transfer tube was retracted from the plasma [4]. At that time, the linear motion slide was at the limit of its travel. The source was opened and the transfer tube repositioned so that it could be further retracted. The results of the subsequent tests of charge breeding efficiency versus transfer tube position are shown in Fig. 2. The tests took place in three series over the course of several years, but the trend within each data set is clear.

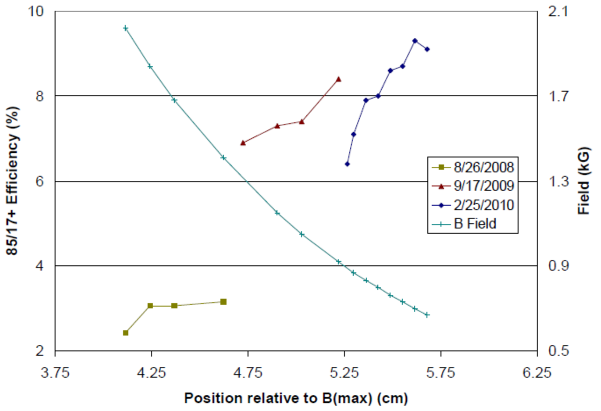

Figure 2: Efficiency of $^{85}Rb^{17+}$ as a function of the transfer tube position. The position is defined as the distance from B_{max} to the end of the transfer tube.

All data sets are taken with a $^{85}Rb^{17+}$ beam provided by a surface ionization source. The source was optimized at each tube position for maximum efficiency in Rb^{17+}. In general, the parameters which were adjusted were the einzel lens, the injection side solenoid, and the ΔV voltage. The tube position is defined as the distance from B_{max} to the end of the transfer tube.

Efficiency Versus ΔV

During charge breeding, the 1+ source and the ECR source are biased with the same power supply. An additional 'tweaker' power supply is in series with the ECR source providing a ΔV voltage, either positive or negative depending on the particulars of the 1+ source, which serves to decelerate the 1+ ions into the ECR plasma. With solid elements (Cs and Rb), it was found that the optimum ΔV was -15 V with a narrow acceptance window of ~5 V. For the gaseous elements (Kr and Xe), the optimum ΔV was +10 V with a very large acceptance window as shown in Fig. 3. There is a steep drop-off in efficiency between +20 and +30 V where the incoming 1+ ions are repelled by the potential and do not enter the plasma chamber. On the other side of the curve, the ions are too energetic and pass through the plasma. However, unlike the solid elements which stick to the cold plasma chamber walls, the gaseous elements are re-emitted and some are charge bred albeit with a lower efficiency and almost certainly a longer hold up time.

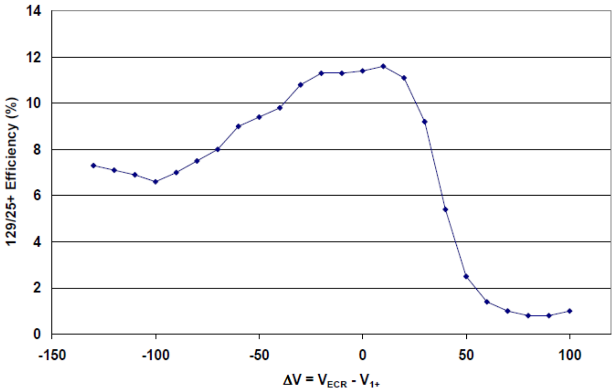

Figure 3: Efficiency of $^{129}Xe^{25+}$ as a function of ΔV.

Multiple Frequency Heating

The effect of multiple frequency heating on the breeding efficiency was previously tested with Cs-133 and Rb-85 with moderate success [4]. These tests were continued with Xe-129 provided by the RF discharge source utilizing a 98% enriched Xe-129 sample. A travelling wave tube amplifier (TWTA) provided RF between 11-13 GHz in addition to a 10.44 GHz klystron. The total RF power was kept constant to serve as a direct comparison of the various RF injection schemes.

With the source running on an oxygen plasma and an extraction voltage of 20 kV, a 65 nA beam of $^{129}Xe^{+}$ was injected into the ECR charge breeder and the breeding efficiency measured as a function of RF power distribution with the results shown in Fig. 4. There is a clear shift in the peak of the charge state distribution when going from single to two-frequency heating. In addition, the global efficiency improved – 42% for 10.44 GHz alone, 46% for 11.90 GHz, and 50% for 10.44+11.90 GHz. In the best configuration, with 350 W of RF injected, the global efficiency was 63% with a maximum efficiency of 13.4% into $^{129}Xe^{25+}$.

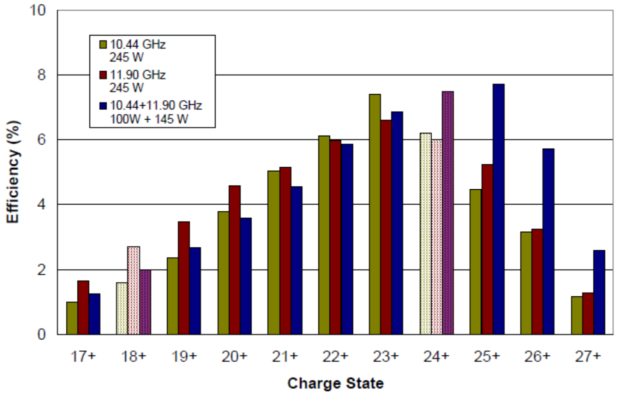

Figure 4: Efficiency of Xe-129 as a function of RF power distribution. The total amount of RF power launched into the source was kept constant. Charge states 18+ and 24+ were obscured by intense background peaks.

Krypton Charge Breeding

A similar set of tests were performed with Kr-86. With the source running on an oxygen plasma at 25 kV extraction, a global efficiency of 77% was observed with a maximum single charge state efficiency of 15.6% into $^{86}\mathrm{Kr}^{17+}$. An efficiency spectrum is shown in Fig. 5 with the shaded columns indicating charge states which could not be observed due to interference peaks. Their values are inferred by the general shape of the distribution.

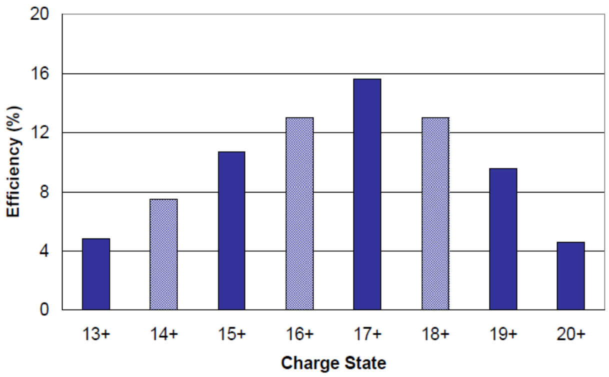

Figure 5: Efficiency spectrum of Kr-86 with the shaded columns indicating charge states which could not be directly observed due to interference peaks.

DISCUSSION

The results in Table 1 demonstrate that the typical relationship of solid elements being half as efficient as gaseous ones is not observed. While not achieving the same level of efficiency as the Kr and Xe, the Rb efficiency is still within a few percent of the gaseous elements. The low breeding efficiency for Cs is attributed to the surface ionization source failing during the testing period. The injection optics could not be optimized, and this led to the reduced efficiency.

A possible explanation for the observed behaviour lies in the design of the 1+ injection region, specifically the iron plug. With shifting the RF injection to the radial ports, a symmetrical magnetic field was maintained in the injection region, whereas with axial RF injection, the waveguide cut-outs introduce a field asymmetry, as shown in Fig. 6 where the center of the magnetic field does not align with the center of the charge breeder and transfer tube. This can introduce steering effects which negatively impact the 1+ injection (particle tracing calculations are being performed to study this hypothesis). It is suggested that the incoming 1+ particles are steered towards the plasma chamber wall before entering the plasma region. In the case of gaseous elements, this is less of an issue due to their not condensing onto the walls of the plasma chamber. However, for solid elements, this would mean that those incoming particles that do impact the wall are lost to the plasma.

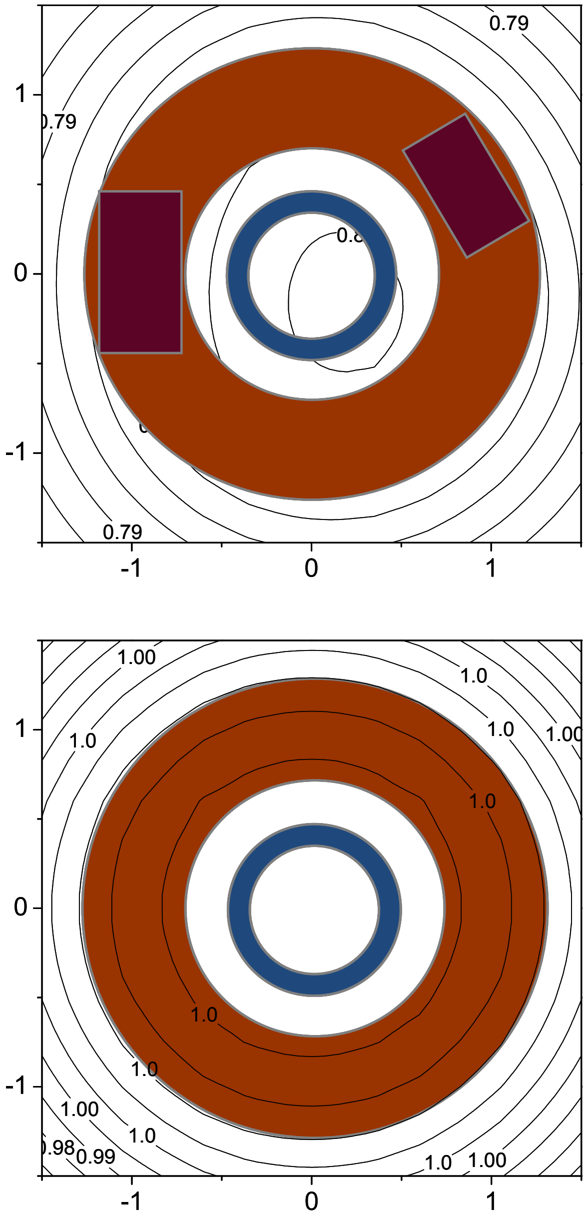

Figure 6: The magnetic field in the injection region with the waveguide cut-outs on top and without on bottom. The overlaid shapes show the position of the transfer tube in blue, the iron plug in brown, and the waveguides in red.

The observed global efficiencies (77% for Kr-86 and 57% for Rb-85) are consistent with a very efficient injection and capture of the 1+ ions. The higher efficiencies for Kr and Xe continue to support the wall recycling model for gaseous elements.

REFERENCES

[1] R. Pardo *et al.*, NIM-B 261, Issues 1-2 (2008) 965.

[2] R. C. Vondrasek, R. Scott, J. Carr, R. C. Pardo, Rev. Sci. Instrum. 79, 02A901 (2008).

[3] R. Geller, Rev. Sci. Instrum. 71, (2000) 612.

[4] R. Vondrasek *et al.,* Rev. Sci. Instrum. 81, 02A907 (2010)